Int J Clin Exp Pathol 2014;7(5):2056-2067
www.ijcep.com /ISSN:1936-2625/IJCEP0000146

Original Article

Electron microscopic features of brain edema in rodent cerebral malaria in relation to glial fibrillary acidic protein expression

Sumate Ampawong[1], Urai Chaisri[1], Parnpen Viriyavejakul[1], Apichart Nontprasert[2], Georges E Grau[3], Emsri Pongponratn[1]

[1]Department of Tropical Pathology, Faculty of Tropical Medicine, Mahidol University, 420/6, Ratchawithi Road, Ratchathewi, Bangkok, 10400, Thailand; [2]Department of Clinical Tropical Medicine, Faculty of Tropical Medicine, Mahidol University, 420/6, Ratchawithi Road, Ratchathewi, Bangkok, 10400, Thailand; [3]Department of Pathology, Faculty of Medicine and Bosch Institute, University of Sydney, 92-94, Parramatta Road, Camperdown, NSW, 2050, Australia

Received March 3, 2014; Accepted April 4, 2014; Epub April 15, 2014; Published May 1, 2014

Abstract: The mechanisms leading to cerebral malaria (CM) are not completely understood. Brain edema has been suggested as having an important role in experimental CM. In this study, CBA/CaH mice were infected with *Plasmodium berghei* ANKA blood-stage and when typical symptoms of CM developed on day 7, brain tissues were processed for electron-microscopic and immunohistochemical studies. The study demonstrated ultrastructural hallmarks of cerebral edema by perivascular edema and astroglial dilatation confirming existing evidence of vasogenic and cytogenic edema. This correlates closely with the clinical features of CM. An adaptive response of astrocytic activity, represented by increasing glial fibrillary acidic protein (GFAP) expression in the perivascular area and increasing numbers of large astrocyte clusters were predominately found in the CM mice. The presence of multivesicular and lamellar bodies indicates the severity of cerebral damage in experimental CM. Congestion of the microvessels with occluded white blood cells (WBCs), parasitized red blood cells (PRBCs) and platelets is also a crucial covariate role for CM pathogenesis.

Keywords: Electron microscope, brain edema, rodent cerebral malaria, glial fibrillary acidic protein (GFAP)

Introduction

The most widely studied murine cerebral malaria (CM) model is *Plasmodium berghei* ANKA (PbA) in CBA or C57BL/6 mice [1]; it results in cerebral syndromes seven days post infection [2]. The pathogenic mechanisms underlining the occurrence of cerebral lesions are still incompletely understood, but may result from accompanying microvessel obstruction and inflammation [3]. A fatal outcome generally depends on sequestration of activated blood cells particularly monocytes and macrophages, parasitized erythrocytes, and platelets in the cerebral vessels [1] consequence of increased pinocytotic activity occurring in the endothelial cells, associated with degenerative changes in the basement membrane and perivascular astrocyte swelling and contributes to the appearance of a perivascular edema [4]. The mouse model of CM, in which cerebral edema appears to play an important role, bears more resemblance to the CM observed in African children than that in South East Asian adults [5]. Maegraith and Fletcher demonstrated excessive movement of water and proteins into the brain of *P. berghei*-infected rodents [6]. Damage to the blood brain barrier (BBB) in *P. berghei*-infected mice was detected, which led to endothelial lesions, edema, and hemorrhage [4, 7].

The two main types of brain edema are cytogenic and vasogenic [8]. Vasogenic edema involves accumulation of excess fluid in the extracellular space of the brain parenchyma because of a leaky BBB [9]. Cytogenic edema consists of intracellular fluid accumulation that occurs during anoxia generating conditions

such as hypoxia [10]. Both cytogenic and vasogenic edema are predominant features of experimental CM [4], however evidence of these in experimental CM has yet not been demonstrated by quantitative electron microscopic study.

Astrocytic swelling is also seen in vasogenic edema. One function of this swelling appears to be uptake of the extravasated plasma protein [11]. Perivascular astrocyte swelling contributes to the appearance of a cytogenic edema seen in reactive astrogliosis, in which the cell cytoplasm is packed with glial fibrillary acidic protein (GFAP) [12]. It is believed that the astrocyte is the major cell type showing swelling after ischemia and trauma [13]. Astrocyte swelling may be an important early event predisposing the brain to further damage, because of the impairment of protective homeostatic mechanisms [14].

Considering the evidence of a causal relationship between brain edema and GFAP expression in experimental CM, this study set out to compare CM-susceptible mice; CBA/CaH mice (CM) and CM-non susceptible mice; BALB/cA mice (non-CM) that inoculated with *P. berghei* ANKA (PbA). This study was designed to compare the evidence of astrogliosis and perivascular GFAP expression between CM and non-CM mice using immunohistochemical study. Fine morphological structure in the perivascular space and within vessels of CM and non-CM mice was also evaluated using an ultrastructural study. The findings of this study demonstrated the correlation between the evidence of astrogliosis and GFAP expression on CM and explained the pathogenic role of cytogenic and vasogenic brain edema together with other related ultrastructural changes in an experimental CM model.

Materials and methods

Animals and parasites

Animal studies were conducted in accord with guidelines under of the Australian Code of Practice for the Care and Use of Animals for Scientific Purposes, and were approved by the University of Sydney Animal Ethics Committee. 14 female CBA/CaH mice (CM) and 15 female BALB/c mice (non CM) (8-10 weeks old) were used in this study, 3 of each were used as controls and 11 CBA/CaH (CM) and 12 BALB/c (non CM) that were infected with *P. berghei* ANKA by intraperitoneal injection of 10^6 parasitized erythrocytes, as described in Grau et al. [15]. The mice were housed in individual ventilation cages and fed *ad libitum* in the laboratory animal facility of the Department of Pathology, University of Sydney. The mice were screened daily for neurological manifestations.

Specimen processing

Mice were euthanized with an over dose inhalation of Isoflurane® on 7 days post inoculation, when the mice showed terminal-stage of severe cerebral complications, including convulsions, paralysis, and coma [16]. A median cranial incision of the brain was done. All specimens were fixed in 10% neutral buffer formalin for 8-h, at 4°C [17]. Fixed specimens were dehydrated and infiltrated using standard tissue processing. The tissues were embedded in paraffin and sectioned at 5 μm. The continuous tissue sections were mounted on SuperFrost Plus slides (Menzel GmbH & Co KG, SF41296PL) for the immunohistochemistry study.

Immunohistochemistry for GFAP

Heat-induced antigen retrieval with citrate buffer, pH 6 was used to unmask the antigen. Endogenous peroxidase was quenched with 1% v/v hydrogen peroxide in methanol after sections were cooled. Sections were washed with 0.2% v/v Tween in Tris buffered saline (TBS) and blocked with 10% w/v skimmed milk for 20 min. Sections were incubated for 30 min at room temperature with 1:40 rabbit anti-GFAP (Biogenex, San Ramon, CA, USA) diluted in TBS with 1% v/v normal goat serum (NGS, Vector, USA, S1000). The sections were washed in TBS and incubated for 30 min with 1:200 biotinylated goat anti-rabbit antibodies (Vector, USA, BA1000) in 1% NGS/TBS at room temperature. The slides were washed, incubated with avidin biotin peroxidase complex (ABC Vectastain, Vector, USA, PK4000) in TBS for 30 min at room temperature, and visualized with diaminobenzidine (DAB, DAKO, K3468). Slides were counterstained with hematoxylin before permanent mounting with Vectamount (Vector, USA).

Quantitative immunohistochemistry analysis

In each group, multiple random fields were examined for a total of 100 microvessels. From each specimen, color images of 640 × 480

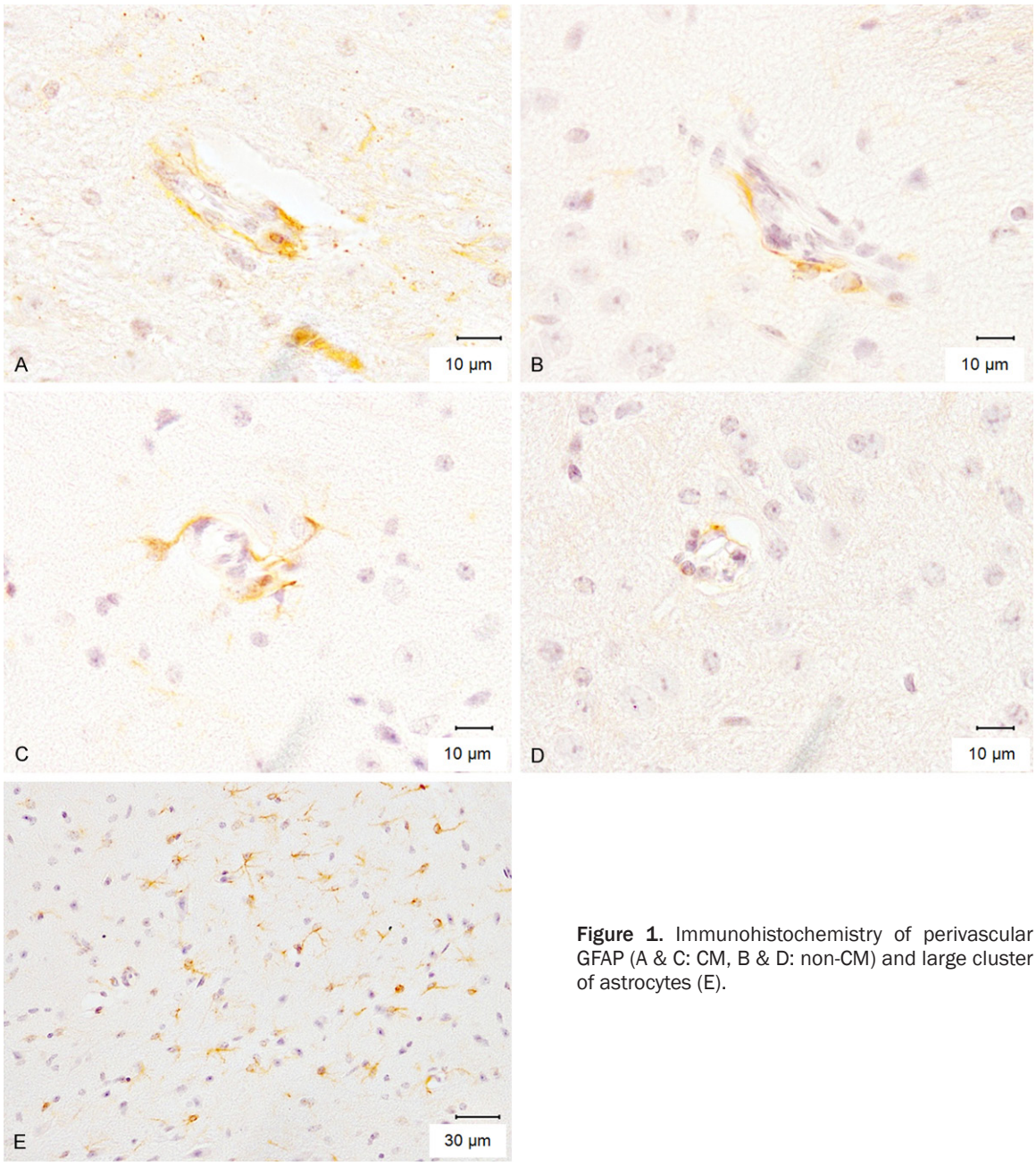

Figure 1. Immunohistochemistry of perivascular GFAP (A & C: CM, B & D: non-CM) and large cluster of astrocytes (E).

pixel resolution (at 400X) were acquired with a light microscope (BX51, Olympus®) and digital camera (DP70, Olympus®). GFAP expression, microvessel labeling, was then analyzed by semi-quantitative digitalized image analysis using analySIS FIVE, Olympus® as described by Kaczmarek et al. and Ampawong et al. [18, 19]. Color images were adjusted, turning the color of non-interesting area to white by replace color mode. Adjusted images were converted to grey-scale images. Then, the area of positive reaction was estimated by the number of black pixels. Thus, the area fraction of the positive reaction was determined as the percentage of black pixels in the binary image.

All of the obvious astrocytic cells were included for counting. The measurement was applied to all areas to determine the number of astrocytic clusters that could be classified as small (astrocytic number < 5 cells/cluster) and large cluster (astrocytic number ≥ 5 cells/cluster).

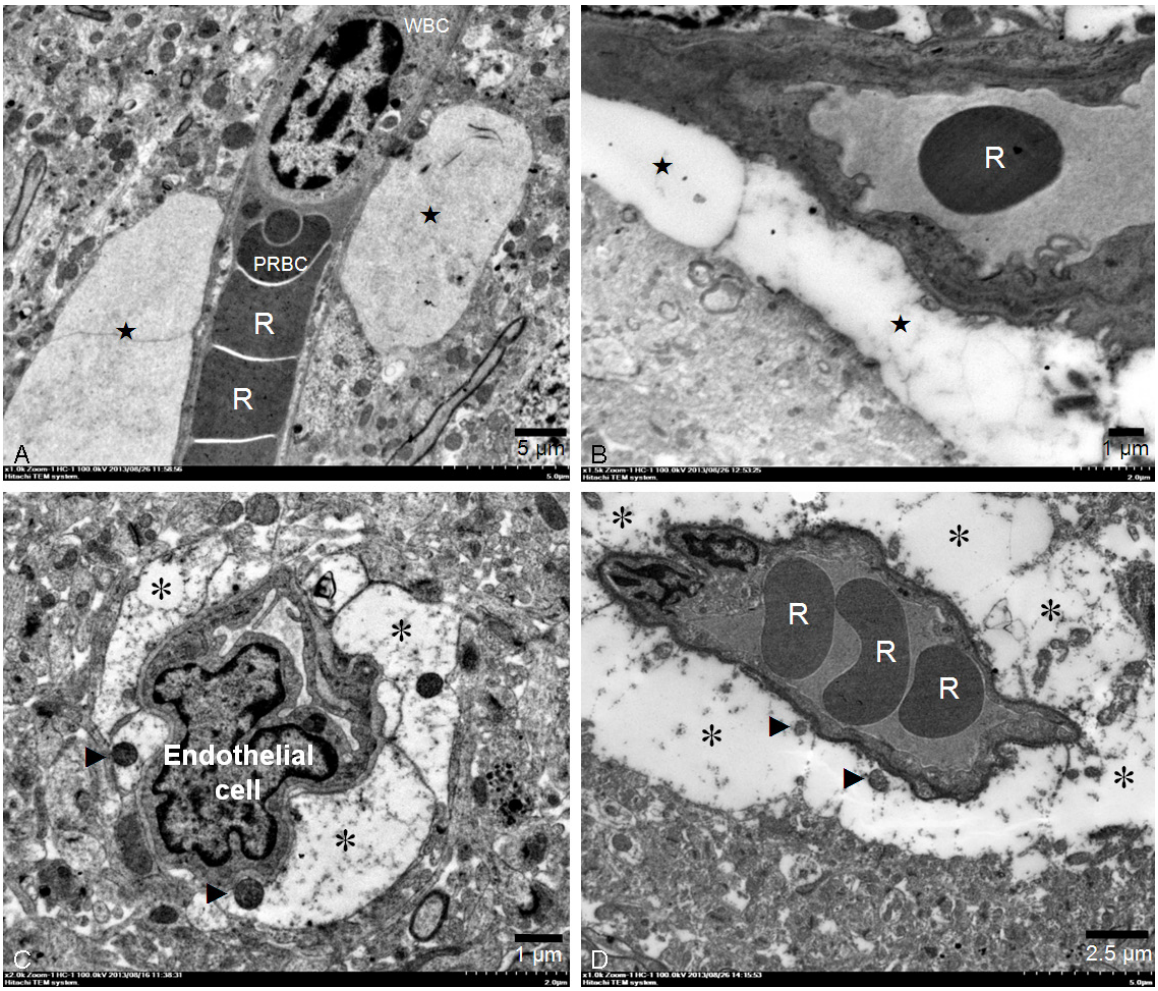

Figure 2. Electron micrographs of perivascular edema and astroglial dilatation. Perivascular edema (★), A: CM and B: non-CM. Astroglial dilatation (*), C: CM and D: non-CM, microvessicular body (►).

Electron microscopy

After euthanizing the mice with an overdose inhalation of Isoflurane® on day 7 post inoculation, specimens were collected from four areas of the brain: cerebellum, cerebrum, brainstem, and the remaining area which composed of midbrain or colliculum hippocampus, and diencephalons. Tissues were then fixed in 2% glutaraldehyde in 0.1 M phosphate buffer, pH 7.4, post-fixation with 1% osmium tetroxide in 0.1 M phosphate buffer, pH 7.4, dehydrated in a graded ethanol series, infiltrated with propylene oxide, and embedded in Spurr's epoxy resin (TABB Laboratories, Reading, UK). Thin sections were cut with glass knives on an ultramicrotome. Copper grids (200-mesh squares) (Agar Scientific, Stansted, UK) were used to collect the thin sections, which were stained with uranyl acetate and lead citrate before electron microscopic examination [20].

Quantitative ultrastructural analysis

Qualitative examinations of pathologic features from these samples were performed as described in Pongponratn et al. [20]. In the perivascular space, the presence of perivascular edema, astroglial dilatation, and multivesicular and lamellar bodies in the astrocytes were examined. Within the vessels, the nature and severity of the following changes were recorded by counting the vessels showing sequestered white blood cells (WBCs), parasitized red blood cells (PRBCs), and platelets. Endothelial cells were assessed for pseudopodia formation, cell swelling, vacuolation, changes in organelle structure, and intercellular bridges. These fea-

Table 1. Presence of perivascular edema in four different brain areas comparing CM and non-CM groups

Brain area	CM: % (+ve/vessel counted)	Non-CM: % (+ve/vessel counted)	*P* value
Cerebrum	42.6 (40/94)	31.3 (20/64)	0.049
Cerebellum	69.4 (43/62)	15.9 (11/69)	0.000
Brain stem	65.7 (23/35)	17.6 (12/68)	0.000
Remaining	49.0 (24/49)	18.8 (9/48)	0.000
Total	54.2 (130/240)	20.8 (52/249)	0.000

Table 2. Presence of astroglial dilatation in four different brain areas comparing CM and non-CM groups

Brain area	CM: % (+ve/vessel counted)	Non-CM: % (+ve/vessel counted)	*P* value
Cerebrum	57.4 (54/94)	18.8 (12/64)	0.000
Cerebellum	22.6 (14/62)	24.6 (17/69)	0.839
Brain stem	54.3 (19/35)	22.1 (15/68)	0.002
Remaining	16.3 (8/49)	60.4 (29/48)	0.000
Total	39.5 (95/240)	29.3 (73/249)	0.020

tures were examined in four different areas of the brain per group. Electron micrographs were taken of relevant areas.

Statistical analysis

Data analysis used IBM® SPSS® statistical software version 20. To determine the level of GFAP expression in each group, Kruskal-Wallis test was used. Pearson's correlation test was used to determine any correlations among variables of interest. Chi-square test with Yates' correction and Fisher's exact test were used to compare between four different brain areas of CM-susceptible mice (CM) and CM-non susceptible mice (non-CM).

Results

GFAP

The perivascular GFAP expression pattern in CM mice (**Figure 1A** and **1C**) was significantly higher than in non-CM mice (**Figure 1B** and **1D**) (13.50 ± 1.57 and 9.75 ± 1.00, respectively) and the number of small astrogliosis clusters were identical in both groups (5.0 ± 4.00 and 5.1 ± 3.00). However the number of large astrogliosis clusters (**Figure 1E**) in the CM mice was significantly higher than in the non-CM mice (6.2 ± 2.00 and 4.2 ± 3.50). There was a positive correlation between perivascular GFAP expression and the presence of large astrogliosis clusters to CM with Pearson's correlation coefficient 0.239 and 0.312 at *p*-values 0.001 and 0.004.

Fine morphology in the perivascular space

Brain edema can be identified by perivascular space and astroglial dilatation (**Figure 2**) which were frequently observed in this study. The results showed that perivascular space and astroglial dilatation in the brains of CM mice (54.2%; 130/240 vessels, 39.5%; 95/240 vessels, respectively) were significantly higher than in those from non-CM mice (20.8%; 52/249 vessels and 29.3%; 73/249 vessels, respectively), with *p*-values of 0.000 and 0.020, respectively. Perivascular edema in all investigated areas was significantly more pronounced in CM than non-CM mice (**Table 1**), while astroglial dilatation was only significantly higher in cerebrum and brain stem (**Table 2**). There was a positive correlation between the presence of perivascular space and astroglial dilatation to CM (Pearson's correlation coefficient 0.344 and 0.108: *p*-value 0.000 and 0.017 respectively).

The fine morphological structure of secondary lysosome which may indicate severity brain damage could be identified by multivesicular and lamellar bodies in their advanced stages (**Figure 3A** and **3B**). The numbers of secondary lysosomes among the groups of CM and non-CM were significantly different. Multivesicular bodies in the non-CM mice (27.3%; 68/249) were significantly higher than in the CM mice (17.5%; 42/240), in contrast with, number of lamellar bodies, which was significantly greater in the CM mice (18.8%; 45/240) than the non-CM mice (9.6%; 24/249). The features of the secondary lysosomes in each area of the brain are detailed in **Tables 3** and **4**. There is a positive correlation between the presence of lamellar bodies to CM (Pearson's correlation coefficient 0.131: *p*-value 0.004), while there was a negative correlation between the presence of multivesicular bodies and CM (Pearson's correlation coefficient -0.117: *p*-value 0.009).

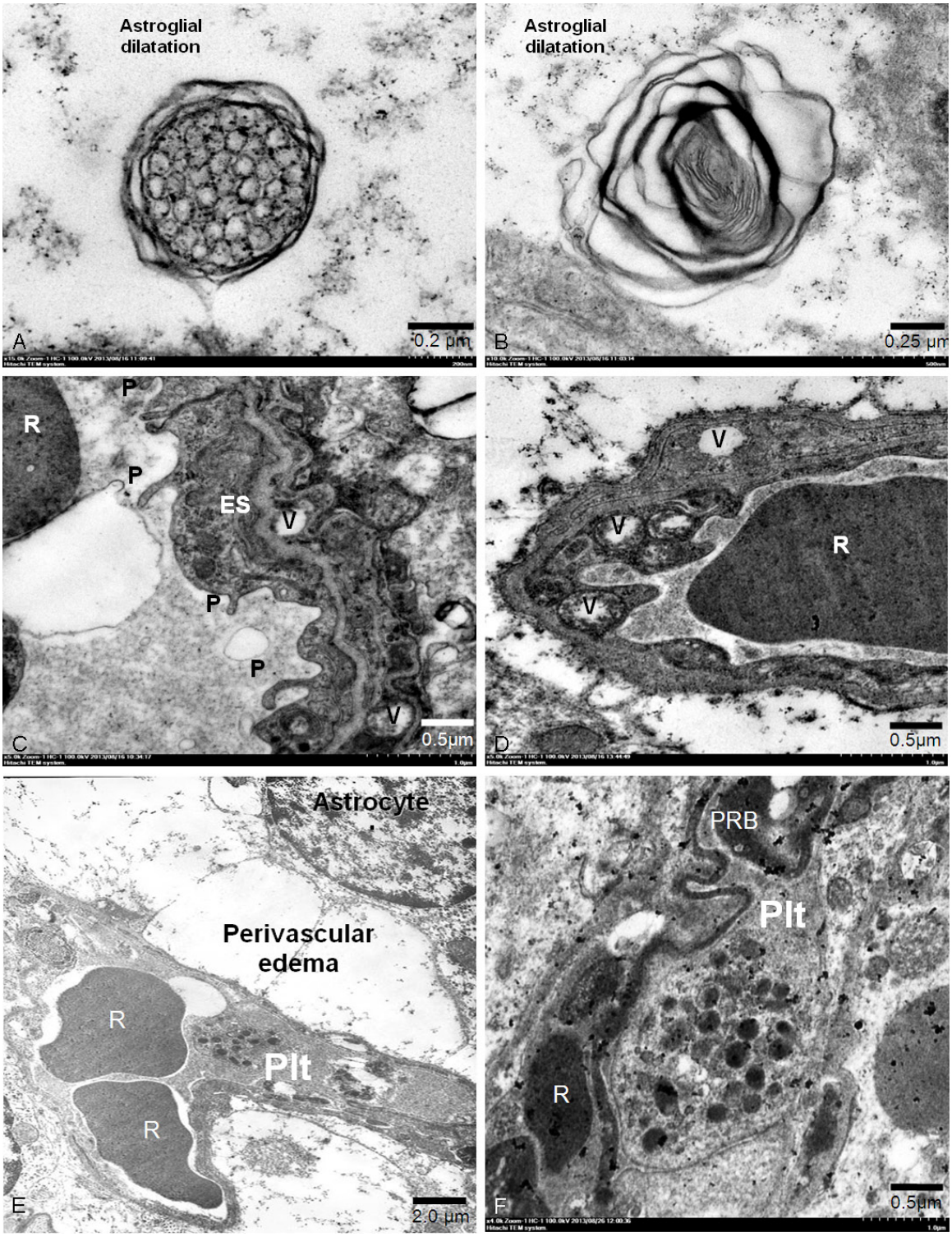

Figure 3. Fine morphological structure of secondary lysosome. A: A multivesicular body is round to oval containing more small vesicles and limited by a double membrane. B: A lamellar body is round to oval containing lots of thin electron dense lamellae and limited by a double membrane. Fine morphological structure of endothelial cell changes: C & D: (P = pseudopodia formation, R = erythrocyte, V = vacuolation, ES = endothelial cell swelling). Fine morphological structure of platelets in brain microvessel: E & F: E: The vascular occluded by red blood cells and platelets with the presence of perivascular edema. F: Evidence of platelets in the cerebral microvessels. (R = erythrocyte, Plt = platelet, PRBC = parasitized red blood cell).

Table 3. Presence of multivesicular bodies in 4 different parts comparing CM and non-CM groups

Brain area	CM: % (+ve/vessel counted)	Non-CM: % (+ve/vessel counted)	*P* value
Cerebrum	25.5 (24/94)	17.2 (11/64)	0.246
Cerebellum	21.0 (13/62)	18.8 (13/69)	0.828
Brain stem	8.6 (3/35)	22.1 (15/68)	0.106
Remaining	4.1 (2/49)	60.4 (29/48)	0.000
Total	17.5 (42/240)	27.3 (68/249)	0.006

Table 4. Presence of lamellar bodies in 4 different parts comparing CM and non-CM groups

Brain area	CM: % (+ve/vessel counted)	Non-CM: % (+ve/vessel counted)	*P* value
Cerebrum	23.4 (22/94)	7.8 (5/64)	0.010
Cerebellum	27.4 (17/62)	4.3 (3/69)	0.000
Brain stem	8.6 (3/35)	7.4 (5/68)	1.000
Remaining	6.1 (3/49)	22.9 (11/48)	0.022
Total	18.8 (45/240)	9.6 (24/249)	0.003

Fine morphology within vessels

The cerebral endothelial cell changes in the PbA model included pseudopodia formation, endothelial cell swelling and vacuolization (**Figure 3C** and **3D**). There was no significant difference between CM (23.8%; 57/240, 17.1%; 41/240, 14.2%; 34/240, respectively) and non-CM mice (28.5%; 71/249, 20.5%; 51/249, 20.9%; 34/249, respectively). The presence of those endothelial cell changes in each brain area was also identical in both groups.

Despite the rare evidence of platelets in the examined brains, the presence of platelets in the brain microvessels (**Figure 3E** and **3F**) in the CM group (6.7%; 16/240) showed a significantly higher trend than in the non-CM mice (1.6%; 4/249). The significantly higher numbers of platelets were found in the cerebrums of the CM mice. There was a positive correlation between the presence of platelets and CM (Pearson's correlation coefficient 0.128: *p*-value 0.005).

The presence of PRBCs within cerebral microvessels quantified by electron microscopy showed that non-CM mice (32.1%; 80/249) exhibited significantly higher levels than CM mice (15.8%; 38/240), and this corresponded with percentage of parasitemia on day 6 post infection, when non-CM and CM mice were 20.35% and 11.68%, respectively. PRBCs are devoid of knobs on their surfaces (**Figure 4**). The distribution of PRBCs in all parts of the brain showed a higher trend among all mice of non-CM group.

White blood cell accumulation in the cerebral microvessels (**Figure 5**) was quantified by electron microscopy, it was found that, the presence of WBC per vessel was no identical in both CM and non-CM mice, without any interaction to other cells.

Discussion

All pathologic descriptions of murine CM previously conducted [1, 2, 16, 21-24] show congestion of the microvessels with occluded blood components (especially WBCs, PRBCs, and platelets) adherence to the vascular endothelium, ischemia and hypoxia, loss of vascular cell integrity, hemorrhage, neuronal damage, edema at the terminal stage, focal demyelination, astrocyte response (redistribution, astrogliosis, activation), microglia and perivascular macrophage response. Electron and light microscopic studies have shown that both infected groups are characterized by widespread cerebral endothelial activation, such as swelling, pseudopodia and vacuolization, together with lesions ranging from isolated damage to necrosis.

The role of cerebral edema in the pathogenesis of CM has been debated for decades, and several techniques has been used, including Evans blue dye leakage, MRI (water diffusion coefficient, imaging, perfusion, angiography, spectroscopy), CT scan, fine morphological studies (perivascular vacuolization, astrocytic swelling), immunohistopathological studies (macrophage associated with perivascular edema; CD68, tight junction associated proteins; occludin, claudin, JAM, ZO-1, ZO-2, ZO-3, reactive gliosis and GFAP) [4, 12, 20, 25-31]. This study determines of perivascular spaces and astroglial dilatation and their correlation with the severity of brain edema. The results show that brain edema was significantly greater in CM than in non-CM mice. The distribution of brain edema was observed throughout the brain,

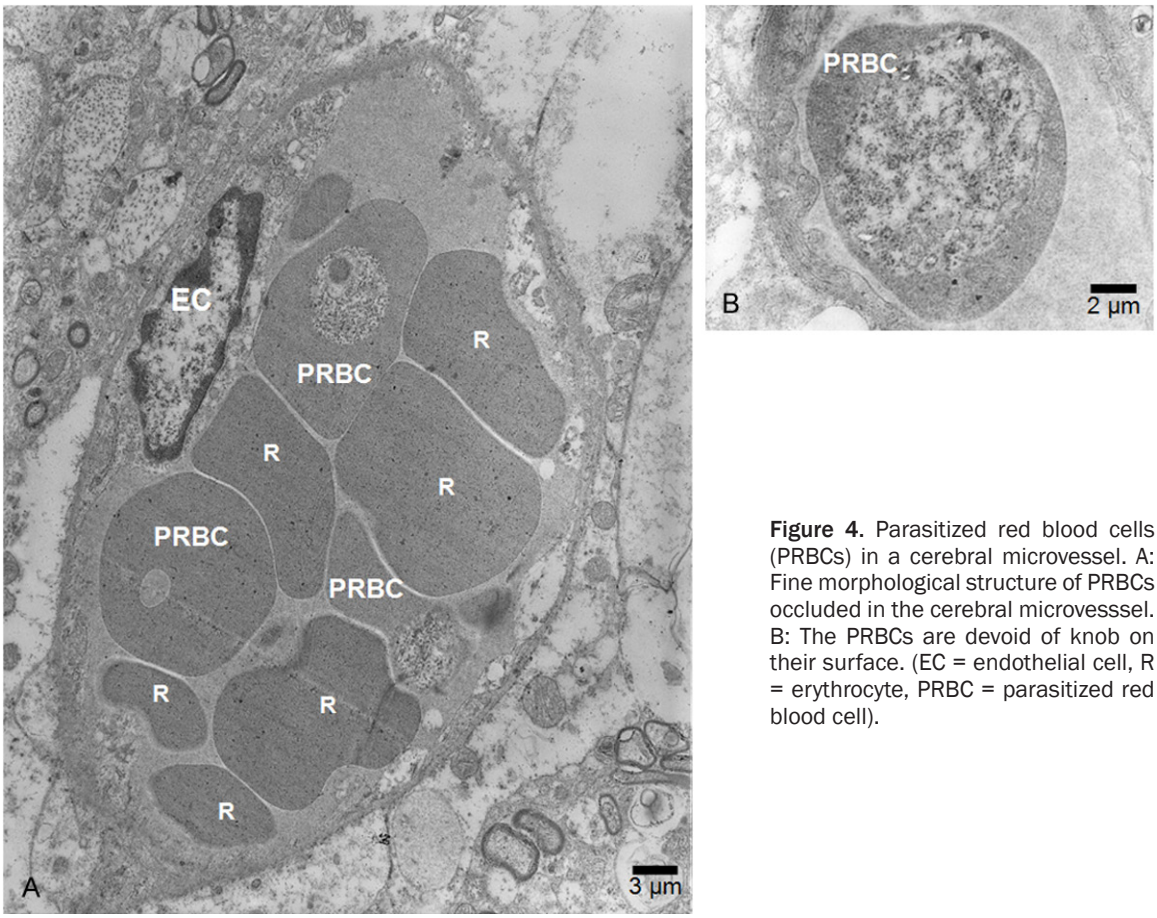

Figure 4. Parasitized red blood cells (PRBCs) in a cerebral microvessel. A: Fine morphological structure of PRBCs occluded in the cerebral microvesssel. B: The PRBCs are devoid of knob on their surface. (EC = endothelial cell, R = erythrocyte, PRBC = parasitized red blood cell).

particularly the cerebrum, brain stem, and diencephalon, in both infected groups. Fine morphological analysis of brain edema regarding the perivascular space and astroglial dilatation confirmed the presence of vasogenic and cytogenic edema. This study also found a positive correlation between the presence of perivascular edema and astroglial dilatation to CM. These data supports the claim that both cytogenic and vasogenic edema are crucial features in experimental CM.

Cytotoxic edema involves an influx of extracellular water into the intracellular compartment leading to cell swelling and irreversible cell damage. It results from anoxic depolarization subsequent to the failure of Na^+/K^+ ATPases to maintain membrane potential after ATP loss [32-34]. It is not considered responsible for brain swelling, because it does not lead to a change in total water content. It is characterized by reduced apparent diffusion coefficient (ADC) value because of con-strained diffusive motion in the extracellular compartment and by impaired energetic metabolism and reduced pH [35]. Vasogenic edema is characterized by expansion of the extracellular compartment after BBB breakdown and relocation of intravascular water into the extravascular compartment. Inflammation is one of the possible mechanisms at the origin of BBB disruption. The result of Penet et al. demonstrate that BBB lesions, brain swelling, and ventricular enlargement play key roles in the development of the cerebral syndrome and confirm the existence of a vasogenic edema [4].

An important role of astrocytes in the normal central nervous system (CNS) is to induce and maintain BBB properties in the vascular endothelium [36]. Astrocytes also make close contact with neuronal synapses and are thought to be intimately involved in maintaining acid-base, electrolyte and neurotransmitter balance [37, 38]. Reactive astrogliosis, which includes an increase in astrocyte size, is actually a hypertrophy of the cells involving increased synthesis of glial filaments and other intracellular constit-

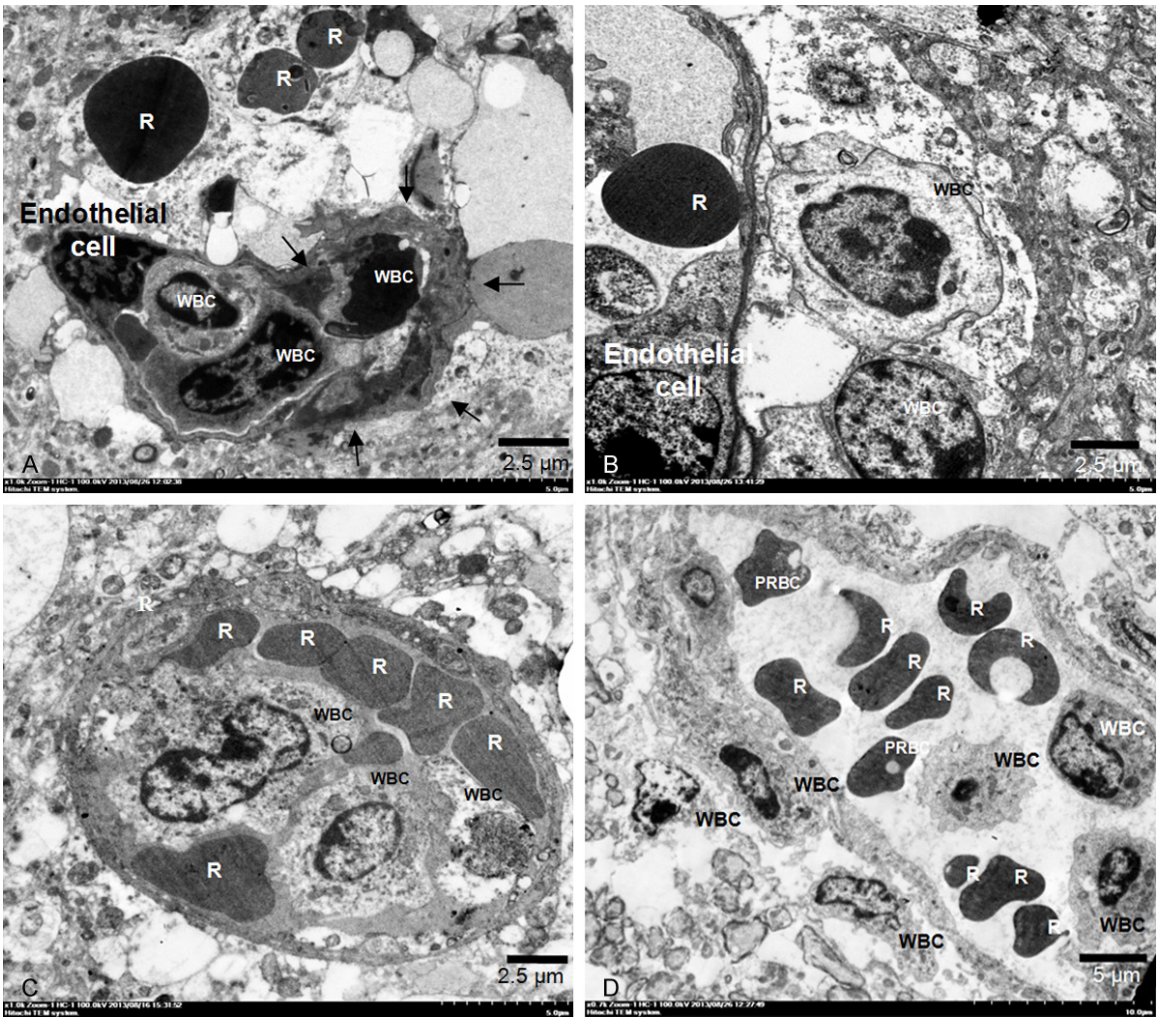

Figure 5. Fine morphological structure of white blood cells (WBCs) accumulation in cerebral microvessel. A: The microvascular occluded with WBCs, exhibiting the area of endothelial damaged (arrow) and surrounded with hemorrhagic area, B: WBCs deposited in perivascular area, C, D: The microvessel accumulated with WBCs, RBCs, and PRBCs. (WBC = white blood cell, R = erythrocyte, PRBC = parasitized red blood cell).

uents associated with increase in size and is usually seen as a delayed response (1-5 days) to injury [14]. This study demonstrates that CM mice had higher GFAP expression in the perivascular area and more large astrocyte clusters than in non-CM mice. Moreover, the correlation between perivascular GFAP expression and the presence of large astrogliosis clusters to CM was positive. These may be an adaptive response of the astrocytes in pathogenesis of CM.

Astroglial swelling during experimental ischemia and trauma in animals has been studied in considerable detail, and is recognized by a pale and watery cytoplasm under electron microscopic analysis [12]. These correspond to the fine morphological features of astroglial dilatation, multivesicular bodies, and lamellar bodies in the astrocyte, which demonstrated that the degenerative level of astrocytes was significantly higher in CM than non-CM mice.

The accumulation of *P. berghei*-infected red blood cells in the brain is crucial for the development of CM in C57BL/6 mice, susceptible strain for CM [39]. PRBCs also accumulate in the brains of PbA-infected CBA/CaH mice, although this is less marked than in other murine models [2]. Therefore PRBCs themselves are an important factor for the cascade of pathological processes in CM.

In addition to PRBC and leukocyte accumulation in the brain microvasculature, platelets

also seem to contribute to neurovascular lesions in murine CM. Wassmer et al. reviewed four lines of evidence supporting platelet involvement in murine CM [40]. (i) electron microscopic analysis when of CM disclosed platelets in the lumen of brain venules, between sequestered monocytes and PRBCs (ii) platelets sequestered in the brain during CM but not in non-CM mice (iii) in vivo treatment with a monoclonal antibody to leukocyte function-associated antigen-1 (which is expressed on platelets) selectively abrogates the cerebral sequestration of platelets, and this correlates with prevention of CM, (iv) malaria-infected animals rendered thrombocytopenic are significantly protected against CM. In this study, although fine morphological analysis showed that the accumulation of platelets in the brain microvessels is significantly more important in CM than in non-CM mice, interestingly the occurrence of platelets in the brain microvessels was quite rare, at 16/240 and 4/249 (+ve/vessels) in CM and non-CM mice, respectively. A positive correlation between the presence of platelets and CM was found. This supports the idea that platelets play an important role in experimental CM, by acting as effectors of neurovascular lesions as previously described [40, 41].

In conclusion, transmission electron microscopy and immunohistochemistry analysis of the rodent malaria model revealed a pathological alteration particularly brain edema. Brain edema and GFAP expression correlate closely with rodent cerebral malaria model. Perivascular space and astroglial dilatation are evidence confirming of vasogenic edema and cytogenic edema respectively. The presences of lamellar bodies in the astrocyte demonstrate the degenerative level of astrocytes. All morphological studies further support the prominent role for CM pathogenesis giving a better understanding of the relationship between brain edema, astrocytic activity, and CM.

Acknowledgements

This study was supported by Research Grant from the Faculty of Tropical Medicine, Mahidol University, Fiscal Year 2014.

Disclosure of conflict of interest

None.

Address correspondence to: Dr. Emsri Pongponratn, Department of Tropical Pathology, Faculty of Tropical Medicine, Mahidol University, 420/6, Ratchawithi Road, Ratchathewi, Bangkok, 10400, Thailand. Tel: (662) 3069184; Fax: (662) 3069184; E-mail: emsri.pon@mahidol.ac.th

References

[1] Hunt NH, Grau GE. Cytokine: accelerators and brakes in the pathogenesis of cerebral malaria. Trends Immunol 2003; 24: 491-499.

[2] Lou J, Lucas R and Grau GE. Pathogenesis of cerebral malaria: recent experimental data and possible applications for humans. Clin Microbiol Rev 2001; 14: 810-820.

[3] Medana IM, Hien TT, Day NP, Phu NH, Mai NT, Chu'ong LV, Chau TT, Taylor A, Salahifar H, Stocker R, Smythe G, Turner GD, Farrar J, White NJ and Hunt NH. The clinical significance of cerebrospinal fluid levels of kynurenine pathway metabolites and lactate in severe malaria. J Infect Dis 2002; 185: 650-656.

[4] Penet MF, Viola A, Confort-Gouny S, Le Fur Y, Duhamel G, Kober F, Ibarrola D, Izquierdo M, Coltel N, Gharib B, Grau GE, Cozzone PJ. Neurobiology of disease. Imaging experimental cerebral malaria in vivo: significant role of ischemic brain edema. J Neurosci 2005; 10: 7352-7358.

[5] Sanni LA. Hypothesis: The role of cerebral edema in the pathogenesis of cerebral malaria. Redox Report 2001; 6: 137-142.

[6] Maegraith B and Fletcher A. The pathogenesis of mammalian malaria. Adv Parasitol 1972; 10: 49-75.

[7] Thumwood CM, Hunt NH, Clark IA and Cowden WB. Breakdown of the blood-brain barrier in murine cerebral malaria. Parasitology 1988; 96: 579-589.

[8] Klatzo I. Neuropathological aspects of brain edema. J Neuropathol Exp Neurol 1967; 26: 1-14.

[9] Pfister HW, Feiden W and Einhaupl KM. Spectrum of complications during bacterial meningitis in adults. Results of a prospective clinical study. Arch Neurol 1993; 50: 575-581.

[10] Papadopoulos MC, Krishna S, Verkman AS. Research seminar: Aquaporin water channels and brain edema. Mount Sinai J Med 2002; 69: 242-248.

[11] Trachtenberg MC. Brain cell responses to extracellular protein. In: Grossman RG, Gildenberg PL, editors. Head Injury: Basic and clinical aspects. New York: Raven press; 1982. pp: 169-178.

[12] Dietrich WD, Alonso O, Halley M. Early microvascular and neuronal consequences of trau-

matic brain injury: a light and electron microscopic study in rats. J Neurotrauma 1994; 11: 289-301.
[13] Kimelberg HK. Current concepts of brain edema. Review of laboratory investigations. J Neurosurg 1995; 83: 1051-1059.
[14] Kimelberg HKN. Astrocytic responses to central nervous system trauma. In: Salzman SK, Faden AI, editors. The Neurobiology of Central Nervous System Trauma. New York: Oxford University Press; 1994. pp: 193-208.
[15] Grau GE, Piguet PF, Engers HD, Louis JA, Vassalli P and Lambert PH. L3T4+ T lymphocytes play a major role in the pathogenesis of murine cerebral malaria. J Immunol 1986; 137: 2348-2354.
[16] Medana IM, Chaudhri G, Chan-Ling T and Hunt NH. Central nervous system in cerebral malaria: 'Innocent bystander' or active participant in the induction of immunopathology? Immunol Cell Biol 2001; 79: 101-120.
[17] Presnell JK, Schreibman MP. Fixative. Humason's Animal Tissue Techniques. Baltimore: Johns Hopkins University Press, 1997.
[18] Ampawong S, Combes V, Hunt NH, Radford J, Chan-Ling T, Pongponratn E and Grau GE. Quantitation of brain edema and localisation of aquaporin 4 expression in relation to susceptibility to experimental cerebral malaria. Int J Clin Exp Pathol 2011; 4: 566-574.
[19] Kaczmarek E, Gorna A, Majewski P. The techniques of image analysis for quantification immunohistochemistry. Anal Acad Med Bial 2004; 49: 155-158.
[20] Pongponratn E, Turner GD, Day NP, Phu NH, Simpson JA, Stepniewska K, Mai NT, Viriyavejakul P, Looareesuwan S, Hien TT, Ferguson DJ and White NJ. An ultrastructural study of the brain in fatal Plasmodium falciparum malaria. Am J Trop Med Hyg 2003; 69: 345-359.
[21] Grau GE, Fajardo LF, Piguet PF, Allet B, Lambert PH, Vassalli P. Tumor necrosis factor (cachectin) as an essential mediator in murine cerebral malaria. Science 1987; 237: 1210-1212.
[22] Hearn J, Rayment N, Landon DN, Katz DR and de Souza JB. Immunopathology of cerebral malaria: morphological evidence of parasite sequestration in murine brain microvasculature. Infect Immun 2000; 68: 5364-5376.
[23] Hunt NH, Golenser J, Chan-Ling T, Parekh S, Rae C, Potter S, Medana IM, Miu J and Ball HJ. Immunopathogenesis of cerebral malaria. Int J Parasitol 2006; 36: 569-582.
[24] Lackner P, Beer R, Helbok R, Broessner G, Engelhardt K, Brenneis C, Schmutzhard E and Pfaller K. Scanning electron microscopy of the neuropathology of murine cerebral malaria. Malar J 2006; 5: 116.
[25] Ebisu T, Naruse S, Horikawa Y. Discrimination between different types of white matter edema with diffusion-weighted MR imaging. J Magn Res Imag 1993; 3: 863-868.
[26] Jennings VM, Actor JK, Lal AA, Hunter RL. Cytokine profile suggesting that murine cerebral malaria is an encephalitis. Infect Immun 1997; 65: 4883-4887.
[27] Looareesuwan S, Wilairatana P, Krishna S, Kendall B, Vannaphan S, Viravan C and White NJ. Magnetic resonance imaging of the brain in patients with cerebral malaria. Clin Infect Dis 1995; 21: 300-309.
[28] Maneerat Y, Viriyavejakul P, Punpoowong B, Jones M, Wilairatana P, Pongponratn E, Turner GD, Udomsangpetch R. Inducible nitric oxide synthase expression is increased in the brain in fatal cerebral malaria. Histopathology 2000; 37: 269-277.
[29] Medana IM and Turner GD. Human cerebral malaria and the blood-brain barrier. Int J Parasitol 2006; 36: 555-568.
[30] Neill AL and Hunt NH. Pathology of fatal and resolving Plasmodium berghei cerebral malaria in mice. Parasitology 1992; 105: 165-175.
[31] Patankar TF, Karnad DR, Shetty PG, Desai AP and Prasad SR. Adult cerebral malaria: prognostic importance of imaging findings and correlation with postmortem findings. Radiology 2002; 224: 811-816.
[32] Ayata C, Ropper AH. Ischaemic brain edema. J Clin Neurosci 2002; 9: 113-124.
[33] Harris NG, Zilkha E, Houseman J, Symms MR, Obrenovitch TP, Williams SR. The relationship between the apparent diffusion coefficient measured by magnetic resonance imaging, anoxic depolarization, and glutamate efflux during experimental cerebral ischemia. J Cereb Blood Flow Metab 2000; 20: 28-36.
[34] Latour LL, Svoboda K, Mitra PP and Sotak CH. Time-dependent diffusion of water in a biological model system. Proc Natl Acad Sci U S A 1994; 91: 1229-1233.
[35] van der Toorn A, Sykova E, Dijkhuizen RM, Vorisek I, Vargova L, Skobisova E, van Lookeren Campagne M, Reese T and Nicolay K. Dynamic changes in water ADC, energy metabolism, extracellular space volume, and tortuosity in neonatal rat brain during global ischemia. Magn Reson Med 1996; 36: 52-60.
[36] Brightman MW. The anatomic basis of the blood-brain barrier. In: Neuwelt EA, editors. Implications of the Blood-Brain Barrier and its Manipulation. New York: Plenum Co.; 1989. pp: 53-78.
[37] Sykova E, Svoboda J, Simonova Z and Jendelova P. Role of astrocytes in ionic and volume homeostasis in spinal cord during development and injury. Prog Brain Res 1992; 94: 47-56.

[38] Walz W. Mechanism of rapid K(+)-induced swelling of mouse astrocytes. Neurosci Lett 1992; 135: 243-246.
[39] Baptista FG, Pamplona A, Pena AC, Mota MM, Pied S and Vigario AM. Accumulation of Plasmodium berghei-infected red blood cells in the brain is crucial for the development of cerebral malaria in mice. Infect Immun 2010; 78: 4033-4039.
[40] Wassmer SC, Combes V and Grau GE. Pathophysiology of cerebral malaria: role of host cells in the modulation of cytoadhesion. Ann N Y Acad Sci 2003; 992: 30-38.
[41] Coltel N, Combes V, Hunt NH and Grau GE. Cerebral malaria -- a neurovascular pathology with many riddles still to be solved. Curr Neurovasc Res 2004; 1: 91-110.